DR. MARION FISCHER-LE SAUX (Orcid ID : 0000-0002-9567-9444)

Article type   : Original Article

Title

Ancestral acquisitions, gene flow and multiple evolutionary trajectories of the type three

secretion system and effectors in *Xanthomonas* plant pathogens

Authors

Déborah Merda[a], Martial Briand[a], Eran Bosis[b], Céline Rousseau[a], Perrine Portier[a], Matthieu

Barret[a], Marie-Agnès Jacques[a]§, and Marion Fischer-Le Saux[a]§

[a]IRHS, Agrocampus-Ouest, INRA, Université d'Angers, SFR 4207 QuaSaV, 49071,

Beaucouzé, France

[b]Department of Biotechnology Engineering, ORT Braude College, Karmiel 2161002, Israel.

§ authors for correspondence.

Correspondence: Marie-Agnès Jacques, marie-agnes.jacques@inra.fr and Marion Fischer-

Le Saux, marion.le-saux@inra.fr ; Fax : +33 2 41 22 57 55

Running title

Evolution of the T3SS in *Xanthomonas*

Abstract

Deciphering the evolutionary history and transmission patterns of virulence determinants is necessary to understand the emergence of novel pathogens. The main virulence determinant of most pathogenic proteobacteria is the type three secretion system (T3SS). The *Xanthomonas* genus includes bacteria responsible for numerous epidemics in agroecosystems worldwide and represents a major threat to plant health. The main virulence factor of *Xanthomonas* is the Hrp2 family T3SS, however this system is not conserved in all strains and it has not been previously determined whether the distribution of T3SS in this bacterial genus has resulted from losses or independent acquisitions. Based on comparative genomics of 82 genome sequences representing the diversity of the genus, we have inferred three ancestral acquisitions of the Hrp2 cluster during *Xanthomonas* evolution followed by subsequent losses in some commensal strains and re-acquisition in some species. While mutation was the main force driving polymorphism at the gene level, inter-species homologous recombination of large fragments expanding through several genes shaped Hrp2 cluster polymorphism. Horizontal gene transfer of the entire Hrp2 cluster also occurred. A reduced core effectome composed of *xopF1*, *xopM*, *avrBs2* and *xopR* was identified that may

allow commensal strains overcoming plant basal immunity. In contrast, stepwise accumulation of numerous type 3 effector genes was shown in successful pathogens responsible for epidemics. Our data suggest that capacity to intimately interact with plants through T3SS would be an ancestral trait of xanthomonads. Since its acquisition T3SS has experienced a highly dynamic evolutionary history characterized by intense gene flux between species that may reflect its role in host adaptation.

Introduction

Unraveling the evolution and transmission of virulence factors is crucial to understanding how pathogens emerge. Type three effectors (T3Es) of Gram negative bacteria are major virulence factors in interactions with both plant and animal hosts. These proteins are secreted directly in host cells by the type three secretion system (T3SS) which is a complex protein structure anchored in the bacterial membrane (Diepold & Armitage, 2015). In pathogenic interactions, T3SS may enable the development of disease (via neutralization of plant defenses and manipulation of host cellular processes) or trigger host resistance (through recognition inducing hypersensitive response). The T3SS is also widespread in mutualistic and commensal bacteria of protist, fungal and animal hosts (Abby & Rocha, 2012). As the T3SS and T3Es play a crucial role in prokaryote-eukaryote interactions, knowledge of their origin and evolution is likely to be crucial to deepen our understanding of host adaptation.

The origin and evolution of the T3SS has been extensively studied and it has been shown to share a common evolutionary history with the flagellar cluster required for swimming motility. Abby and Rocha (2012) recently proposed that the T3SS evolved by exaptation from the flagellar cluster. Further T3SS diversification then lead to seven distinct

families of T3SSs (Ysc, SPI-1, SPI-2, Chlamy, Hrp1, Hrp2 and Rhizo) (Troisfontaines & Cornelis, 2005). Diversification of the T3SS is not explained simply by vertical evolution. Indeed, it was shown that the evolution of the T3SS cluster has included numerous horizontal gene transfers (HGTs) (Troisfontaines & Cornelis, 2005). These HGT events are facilitated by localization of T3SS in plasmids or chromosomal pathogenicity islands.

Extensive diversification of the T3SS seems to be driven by bacteria ecology, as T3SS families correlate with the host type. Indeed, Rhizo, Hrp1 and Hrp2 seem to be more frequently involved in interactions with plants, whereas Ysc, Chlamy, SPI-1 and SPI-2 appear to be specific to interactions with mammals, insects and amoeba (Abby & Rocha, 2012; Diepold & Armitage, 2015; Troisfontaines & Cornelis, 2005). In general, each bacterial genus harbors a T3SS from a specific family but some bacteria with complex lifestyles harbor several T3SS from different families. These contrasting patterns of T3SS content could be explained by ancient vertical inheritance mixed with T3SS gain and loss events (Kirzinger, Butz, & Stavrinides, 2015). The main T3SS families found in phytopathogens are Hrp1 (in *Pseudomonas* and *Erwinia*) and Hrp2 (in *Xanthomonas, Ralstonia, Acidovorax,* and *Burkholderia*), however alternative non-canonical T3SS have also been described in some plant-associated bacteria such as commensal pseudomonads associated with plants (Barret et al., 2013). These two main families of T3SS clusters, Hrp1 and Hrp2, differ in gene content, synteny, and transcriptional regulation. Approximately 20 protein-coding genes, called *hrp* (hypersensitive reaction and pathogenicity) and *hpa* (hrp-associated) genes, are involved in the biogenesis of T3SS. Among them, nine genes, which were renamed *hrc* (hrp conserved), are highly conserved in plant and animal pathogens and eight have homologs in the flagellar cluster (Tampakaki et al., 2010).

T3E repertoires are highly diverse within each genus and even within single bacterial species (McCann & Guttman, 2008). They vary both in terms of content and size, for instance a given *X. axonopodis* strain may have any between six and 26 T3E genes (Hajri et al., 2009). It has been suggested that this high variability could be the consequence of the host adaptation process. Indeed, in *Pseudomonas* and *Xanthomonas*, the pathogenic strains are highly host specific and the T3E repertoire composition is correlated with host range (Hajri et al., 2009; Sarkar, Gordon, Martin, & Guttman, 2006). The plasticity of T3E repertoire within a species could be explained by frequent HGTs (McCann & Guttman, 2008) as many T3E genes have been found associated with mobile genetic elements. Understanding the diversity and evolution of T3E repertoires in pathogenic bacteria is essential to gain insight into host adaptation mechanisms. However, identification of T3E genes in whole genome sequences remains a challenge as T3Es are structurally and functionally highly diverse with more than 50 families identified so far in *Xanthomonas* and *Pseudomonas* (Lindeberg, Cunnac, & Collmer, 2012; Ryan et al., 2011). Recently, machine learning approaches have been developed. They rely on multiple criteria such as the presence of a secretion signal necessary for recognition by T3SS machinery that is found in N-terminal region of T3E (McDermott et al., 2011) or specific amino-acid composition (Lower & Schneider, 2009). In *Xanthomonas*, these approaches have enabled the identification of seven novel T3Es in the reference strain 85-10 (Teper et al., 2016), exhibiting great promise for future discoveries with the exponential growth of genomic data.

Xanthomonas are major plant pathogens, devastating crops worldwide. The major pathogenicity determinants of xanthomonads arethe Hrp2 type-T3SS and its effectors (White, Potnis, Jones, & Koebnik, 2009). *X. albilineans* is an exception in the genus as it has no Hrp2 family gene cluster, but a SPI-1 T3SS (Marguerettaz et al., 2011). Four *Xanthomonas* species lacking any Hrp-T3SSs and associated T3Es, namely *X. sacchari* (Studholme et al., 2011),

"*X. cannabis*" (Jacobs, Pesce, Lefeuvre, & Koebnik, 2015), "*X. pseudalbilineans*" (Pieretti et al., 2015) and *X. maliensis* (Triplett et al., 2015) were recently described. Moreover, some *X. arboricola* strains were also found without any T3SS (Cesbron et al., 2015; Merda et al., 2016). The *X. arboricola* strains lacking any T3SSs are considered commensal, since no pathogenicity on their respective hosts has been observed. The *X. arboricola* species has an epidemic population structure, where epidemic clones are represented by successful pathovars (defined as pathovars responsible for epidemics worldwide). They infect stone and nut fruit trees and the recombinant network is represented by commensal strains and unsuccessful pathovars (defined by a limited geographical and potentially temporal expansion) (Merda et al., 2016). Epidemic clone emergence seems to be correlated with the acquisition of T3Es whereas in the recombinant network, strains would have lost T3E coding genes and the T3SS cluster.

The recent discovery of several *Xanthomonas* species and strains that lack the Hrp2 cluster has raised questions about the evolution of virulence and the origin of the T3SS in this genus. Are pathogenicity and Hrp2 clusters ancestral features of *Xanthomonas* that have been vertically inherited and lost in some species or do they represent more recent acquisitions? Contrasting with our deep knowledge of ancient evolutionary history of T3SS, little is known about recent origin and evolution of T3SS and its role in plant pathogen emergence. Given the pivotal role of T3SS and T3Es in xanthomonads pathogenicity and host specificity, and given their heterogeneous distribution at genus and species scales, the Hrp2 cluster and its effectors in *Xanthomonas* genus appear to be a good model to study T3SS origin and evolution at a fine evolutionary scale. In this study, we conducted our analyses on a collection of strains representing all valid species from the two phylogenetic groups of the genus (group 1 and 2) as defined by Young, Park, Shearman, & Fargier (2008). We inferred their phylogenetic relatedness based on the core genome of the whole genus. Moreover, to get

insights into T3SS evolution, we studied not only cluster synteny, *hrc* gene phylogeny, and homologous recombination, but we also considered the genomic environment of the T3SS cluster. Finally, to unveil the evolution of T3E repertoires in relation with pathogen emergence, we determined the T3E repertoires in a collection of 44 *X. arboricola* genomes representing both commensal and pathogenic strains using a machine learning approach designed to detect T3E coding genes in *Xanthomonas* genome sequences.

Materials and methods

Genome sequencing and annotation

We used a collection of 82 genome sequences (see Data Set S1, Supporting information) representing the diversity of *Xanthomonas* genus (36 strains belonging to *Xanthomonas* spp.) and the known diversity of *X. arboricola* (44 additional strains; 23 strains being commensal and 21 pathogens) (Merda et al., 2016). Genomes were sequenced using the Illumina technology and HiSeq 2500 (Genoscreen, Lille, France) or MiSeq instruments. Libraries of genomic DNA were performed using the Kit Nextera XT (Illumina, USA). Paired-end reads of 2 x 100 bp were assembled in contigs using SOAPdenovo 1.05 (R. Li et al., 2010) and Velvet 1.2.02 (Zerbino & Birney, 2008). Annotation was performed using EuGene-PP (Sallet, Gouzy, & Schiex, 2014).

Prediction of T3SS cluster and T3E repertoires

The T3SS coding genes representing all T3SS families (Ysc, SPI-1, SPI-2, Chlamy, Hrp1, Hrp2, Rhizo) and their diversity were identified in genome sequences using BLASTp searches with the query sequences presented in the Data Set S2 (Supporting information). We included in our search T3SS encoding genes from *Rhizobiales*, *Burkholderiales*, *Ralstonia*, *Bordetella*, *Xanthomonas*, *Pseudomonas*, *Escherichia coli*, *Erwinia*, *Salmonella*, *Shigella*, *Yersinia* and *Chlamydia*. Candidate T3SS genes were assigned to a T3SS family when the percent of identity was higher than 80% on at least 80% of the length of the query sequence. Lower thresholds were used to highlight putative pseudogenes. The T3E gene detection was performed in all genomes of *X. arboricola* by a machine-learning approach adapted from Teper et al. (2016) (E. Bosis, unpublished data, manuscript in preparation).

Genomic environments of genes

The genomic environments flanking and encompassing the T3SS cluster were analyzed using the R package GenoplotR (Guy, Roat Kultima, & Andersson, 2010). BLASTn between contigs encompassing the T3SS cluster were performed and only BLAST hits with e-values below 0.01 were used to highlight conserved regions on the plots. First, this analysis was performed only using strains having a T3SS cluster to detect conserved flanking regions upstream and downstream of the cluster between phylogenetic neighbors. For strains lacking T3SS, a BLASTn search was used to find if regions flanking T3SS in T3SS positive strains were also present in T3SS negative strains. 5 Kb T3SS-flanking regions identified in the closest phylogenetic neighbors of each T3SS negative strain were used as query sequences to identify the contig to use in further analyses. To study the synteny in the genomic environments of T3SS insertion site, both contigs from strains with and without T3SS cluster

were included in the final analysis. Similar genomic environments of T3SS cluster were defined based on synteny and shared conserved regions spreading over at least four CDS in a 20 Kb window at the left and right side of T3SS cluster and using *X. arboricola* CFBP 7179 as a reference (Fig. S1, Supporting information). Similar genomic environments of the T3SS cluster were highlighted with the same colour as shown in Fig. S1 (Supporting information). The same approach but using a 200 Kb window upstream and downstream the cluster was used to define the genomic context of T3SS insertion site. For the genomic environments of T3E genes, these T3E genes were located by their locus tag obtained during the search with the machine learning approach. The same strategy as described above was used to study the genomic environment of *avrBs2* insertion site.

Mapping T3E genes on whole genome sequences

To locate the T3E genes in the genomes of *X. arboricola* pathogenic strains of group A, the contigs of genome sequences were ordered using MAUVE (Darling, Mau, Blattner, & Perna, 2004). The sequence of CFBP 2528 was used as reference because among group A strains of *X. arboricola*, the number of contigs was the lowest for this strain (8 contigs). For each genome, the contigs were concatenated using Geneious (Kearse et al., 2012) according to the order obtained with MAUVE. The circular representations were obtained using DNAPlotter (Carver, Thomson, Bleasby, Berriman, & Parkhill, 2009). The localization of each T3E genes in pathogenic strains was identified using their locus tag.

Determination of core proteomes

The core proteome of *Xanthomonas* was identified with orthoMCL-companion (Carrere, Cottret, Rancurel, & Briand, 2015). The core proteome of *X. arboricola* was identified with orthoMCL V2.0.9 analyses on predicted full-length proteins (L. Li, Stoeckert, & Roos, 2003). OrthoMCL clustering analyses were performed using the following parameters: P-value Cut-off = 1×10^{-5}; Percent Match Cut-off = 80; MCL Inflation = 1.5; Maximum Weight = 316.

Phylogenies of core and T3SS coding genes

Phylogenies were performed using maximum likelihood in the phyML software package. The phylogeny of the *Xanthomonas* genus was performed using the concatenated core proteome obtained with orthoMCL-companion. For *X. arboricola* phylogeny, the concatenated orthologous groups were used. Each orthologous group in *X. arboricola* was aligned using MACSE (Ranwez, Harispe, Delsuc, & Douzery, 2011). Only alignments with more than 75% sequence identity were kept for the phylogeny reconstruction. These alignments were concatenated using Geneious (Kearse et al., 2012). For organism maximum likelihood phylogenies the JTT model was used. For the T3SS coding genes phylogeny, each *hrc* gene (with the exception of *hrcL* for which some CDS were truncated) was aligned using MUSCLE (Edgar, 2004), taking into account sequence translation in proteins to conserve the reading frame. The 10 *hrc* genes were concatenated according to their order in T3SS cluster. The phylogenic analysis was performed with the GTR + I + gamma model, corresponding to the best model identified by jModelTest (Posada, 2008).

Phylogeny comparisons and recombination analyses

The topology of the concatenated *hrc* tree was compared to the core proteome tree of *Xanthomonas* genus with a Shimodaira-Hasegawa test (Shimodaira & Hasegawa, 1999) implemented in R package phangorn (Schliep, 2011). In the same way, topologies of each individual *hrc/hrp* tree were compared to each other and to the topology of the concatenated *hrc/hrp* tree. The impact of recombination (*r*) relative to mutation (*m*) was analyzed with the *ρ/θ* statistics using RDP v.3.44 (Martin et al., 2010) for each *hrc/hrp* gene located in the core region of the cluster (16 genes between *hrcC* and *hrpE*). The origins of recombinant sequences were identified by examining the concatenated sequences of *hrp* and *hrc* genes (concatenated according to their order in T3SS cluster) using RDP 3, GENECONV, BOOTSCAN, MAXIMUM CHI SQUARE, CHIMAERA, SISCAN, and 3SEQ implemented in RDP v. 3.44 (Martin et al., 2010). We considered that a recombination event was statistically supported when it was detected by at least two methods (Merda et al., 2016). The recombination event representation was visualized using Circos (Krzywinski et al., 2009).

Results

Organism- and T3SS-evolutionary histories in *Xanthomonas*

The presence of T3SS genes was investigated in 82 genome sequences of *Xanthomonas* strains (Data Set S1, Supporting information) through BLASTp searches of 295 proteins representing the diversity of T3SS families (Data Set S2, Supporting information). The Hrp2 cluster was detected in 61 genome sequences, SPI-1 was identified in the genome sequence of *X. albilineans*, and 20 genome sequences were free of any T3SS encoding genes whatsoever, with fourteen of which belonging to *X. arboricola* (12

commensal strains and two strains of the pathovar *populi)*. T3SS clusters were also missing

in *X. pisi* and *X. melonis* genomes, and as previously shown in some "*X. cannabis*" strains, *X.*

maliensis and the group 1 species *X. sacchari*.

A robust phylogenetic tree of the *Xanthomonas* genus, based on the core proteome,

was constructed to provide a reference point to infer evolutionary scenarios of T3SS gains

and losses (Fig. 1). According to this phylogenetic reconstruction, *X. maliensis* and *X.*

campestris diverged very early from other species in group 2. This isolated phylogenetic

position of *X. campestris* clade was unexpected as previous multilocus sequence analyses on

whole genus diversity placed *X. campestris* in the core of group 2 (Triplett et al., 2015;

Young et al., 2008). However, in a genome-based phylogeny of a limited number of species a

similar phylogenetic relationship has been inferred (Naushad & Gupta, 2013; Rodriguez et

al., 2012). Three major clades supported by 100% bootstrap values grouped nearly all other

group 2 species: (i) clade A encompassing *X. arboricola*, *X. gardneri, X. cynarae*, *X.*

hortorum and *X. populi*; *X. fragariae* appeared as an isolated branch at the base of this clade.

(ii) clade B encompassing species of the *X. axonopodis* complex (*ie X. alfalfae*, *X. perforans*,

X. euvesicatoria, X. axonopodis, *X. fuscans* and *X. citri*), *X. oryzae*, *X. vasicola* and *X. bromi*,

and (iii) clade C encompassing "*X. cannabis*", *X. codiaei*, *X. cassavae*, *X. melonis*, *X.*

cucurbitae, *X. pisi*, *X. dyei* and *X. vesicatoria* (Fig. 1). Hrp2-negative strains were

interspersed in the phylogenetic tree of the genus; a distribution pattern that could be either

explained by ancestral acquisition and subsequent losses or by numerous recent independent

Hrp2 acquisitions.

A comparison of upstream and downstream genomic environments (20 Kb on each

side) of the T3SS cluster in the different *Xanthomonas* species allowed us to define similar

genomic environments based on synteny and similarities of DNA fragments (Fig. S1,

Supporting information). Strains exhibiting similar flanking regions around the T3SS cluster

were considered to have vertically inherited a T3SS cluster following a single acquisition event in their common ancestor. This analysis revealed three ancestral acquisitions of this cluster. One of these acquisitions would have occurred in the ancestor of the three group-2 clades (A, B, C). The same genomic environments of Hrp2 clusters were highlighted in strains belonging to clade A and *X. bromi* (clade B) (Figs 1 and S1, Supporting information). Given the divergence between these strains, it is tempting to speculate that Hrp2 cluster was acquired through a single acquisition event in a common ancestor. However, except in the case of clade A and *X. bromi*, the *hrp* cluster was retrieved in several different genomic environments in clades B and C (Figs 1 and S1, Supporting information). Two scenarios could explain this situation: the first scenario involves the loss of the ancestral Hrp2 cluster and re-acquisition at a different genomic context, and the second scenario includes rearrangements in the 20 Kb flanking regions of the ancestral Hrp2 cluster without affecting the genomic context of T3SS insertion site. To decipher which scenario is the most probable, genomic contexts of the T3SS insertion site (*ie* broader genomic environments spreading over 200 kb upstream and downstream) were compared in clades B and C strains selected for the quality of their genome assembly (Figs. 1 and S2, Supporting information). We showed that rearrangements occurred in the direct flanking regions of T3SS cluster of these strains but that the genomic context of T3SS cluster was similar to those of clade A strains and *X. bromi*. Insertions of large fragments (80 kb for *X. euvesicatoria, X. alfalfae* and *X. fuscans* and 50 kb for "*X. cannabis*" strain CFBP 7912) in T3SS flanking regions broke synteny in the 20 kb window but this synteny with the direct genomic environment of *X. bromi* and clade A was observed further away from T3SS cluster in the clade B and C genome sequences. Thus, genomic rearrangement events and gene insertions affected the 20 Kb genomic environment of the T3SS cluster but not its location in the genome; the genomic contexts of T3SS cluster remained similar. These rearrangements differed between different clades and were

sometimes supported by the presence of insertion sequences (ISs) and tRNAs (Figs S1 and S2, Supporting information). Altogether, these results support the hypothesis that there was an ancestral acquisition of the T3SS cluster in the common ancestor of clades A, B, and C and subsequent rearrangements in flanking regions of the Hrp2 cluster (Fig. 1).

The second acquisition most likely occurred in *X. campestris* ancestor. In this clade the T3SS cluster was found in a different genomic context as no synteny could be found even when flanking regions as broad as 200 kb were compared with those of other *Xanthomonas* species (Figs. 1 and S2, Supporting information). The phylogenetic tree of T3SS encoding genes (Fig. 2B) showed that *X. campestris* T3SS genes were phylogenetically related to those of clade A strains. Thus the common ancestor of *X. campestris* might have acquired the *hrp* cluster by HGT from a clade A strain. However, the T3SS encoding genes underwent homologous recombination (see below) that altered the phylogenetic signal of the *hrp* genes. Thus, we can not exclude the possibility that an ancestral *X. campestris hrp* cluster would have been replaced by homologous recombination with a clade A strain. Thus, we favor the most parsimonious scenario of an independent acquisition in *X. campestris* ancestor as opposed to an acquisition by the common ancestor of all group 2 strains followed by the loss of this T3SS cluster in *X. campestris* and its re-acquisition in a different genomic context.

The third acquisition of the T3SS cluster would have occurred in group 1. In this case, the T3SS cluster included the genes encoding the master regulators HrpX and HrpG. In contrast, in group 2 species, these two genes were located outside the T3SS cluster. Moreover, all T3SS encoding genes are highly divergent from those of group 2 strains (Figs 2B and S3, Supporting information). While the genomic environments of the T3SS clusters among group 1 strains shared similarities, the T3SS genomic context had no similarity to those of group 2 strains (Figs 1, S1 and S2, Supporting information). Altogether, this suggests

an independent acquisition event of the T3SS in the common ancestor of *X. translucens*, *X. hyacinthi* and *X. theicola*.

Ancestral acquisitions of T3SS clusters imply that the absence of Hrp2 clusters in the 19 strains of *Xanthomonas* group 2 was the result of multiple loss events. The *X. arboricola* strains lacking T3SSs were dispersed in five monophyletic lineages indicating at least five loss events during diversification of this species (Fig. 1). One loss event could have occurred in the common ancestor of the two strains belonging to "*X. cannabis*" and two independent loss events could have occurred in *X. melonis* and *X. pisi*. As *X. maliensis* was the most divergent species of group 2, it was impossible to hypothesize any event responsible for absence of the T3SS cluster, and this species might have never had any T3SS cluster. In the 19 strains without T3SSs, the entire T3SS cluster was missing. No traces of pseudogenization, which could be identified by a weak homology with T3SS coding genes with a BLASTn approach, were detected. BLASTn searches with the flanking regions of the Hrp2 cluster in strains lacking it and synteny analysis allowed us to identify the probable excision sites of the DNA fragment containing the Hrp2 encoding genes (Fig. S1, Supporting information). Excision would have occurred between *trpG* and *ltaE*. Nevertheless, we did not find any mobile genetic elements between these loci.

A loss followed by a re-acquisition of the whole T3SS cluster should have taken place in the evolutionary history of *X. fragariae* and *X. cassavae*. Despite their phylogenetic positions in *Xanthomonas* group 2, the genomic context of T3SS insertion site was different. Indeed, a lack of synteny in T3SS flanking regions was observed among *X. fragariae, X. cassavae* and other group 2 *Xanthomonas* species, even when flanking regions as large as 200 kb were considered (Figs S1 and S2, Supporting information). Because these species were localized in two different phylogenetic positions within group 2, this suggests independent re-acquisition events (Fig. 1). However, for *X. fragariae*, another hypothesis could be put forth.

The position of this species is similar in the organism- and T3SS phylogenies indicating a probable ancestral T3SS acquisition. In this hypothesis the different genomic context of T3SS could be the result of a transposition of the cluster within *X. fragariae* genome. Four ISs were found upstream and downstream of the T3SS cluster in *X. fragariae* genome that corroborated either transposition or re-acquisition via HGT as a mechanism. As for strains devoid of the T3SS cluster, we looked at the insertion site of the ancestral T3SS acquisition in clades A, B and C and no remnants of the ancestral T3SS cluster were detected at this location. *X. codiaei* shared the same left border of T3SS cluster as *X. cassavae*, its sister species, suggesting that the loss and re-acquisition of T3SS cluster might have occurred in their common ancestor, but unfortunately contig interruption in *X. codiaei* precluded the analysis of a large genomic environment to confirm this hypothesis.

Homologous recombination in the T3SS coding genes

To determine if the T3SS cluster follows the same evolutionary history as the species, a phylogeny based on concatenated *hrc* coding genes was compared to the organism phylogeny based on the core proteome of Hrp2-positive strains (Fig. 2A and B). Numerous incongruences were observed and confirmed by the SH test (*p-value* = 0.00092). For instance, while most *X. arboricola* strains exhibited a monophyly for the T3SS coding genes, T3SS coding genes from the *X. arboricola* pv. *guizotiae* diverged from those of other *X. arboricola* strains (Fig. 2B) and they were closely related to those of "*X. cannabis*" strains CFBP 7912 and Nyagatare. Similar incongruences were observed for *X. campestris*, *X. cassavae, X. codiaei, X. dyei* and *X. vesicatoria* whose T3SS coding genes were phylogenetically related to those of clade A despite the high divergence among these species

in the organism phylogeny. These incongruences between *hrc* phylogeny and organism

phylogeny can be explained by homologous recombination occurring during T3SS evolution.

To determine if recombination events affected the whole cluster or only some genes,

individual phylogenies were built for each *hrc/hrp* gene coding for the T3SS (Fig. S3,

Supporting information). In all phylogenies, *X. arboricola* pv. *guizotiae* strains (CFBP 7408

and CFBP 7409) did not group with other *X. arboricola* strains, but with "*X. cannabis*"

strains CFBP 7912 and Nyagatare, suggesting that their whole T3SS cluster was acquired

through a single homologous recombination event with these phylogenetically distant strains.

Individual *hrc/hrp* phylogenies were compared in pairs using a SH test (Table S1, Supporting

information). For half of the comparisons, the *p-values* were below 0.05, indicating that most

topologies of these trees were significantly different, and that recombination occurred

between *hrc* genes. For instance T3SS coding genes from *X. campestris* clustered with genes

from clades A and C (Fig. 2B and Fig. S3, Supporting information) that did not reflect the

intermediate position of *X. campestris* between group 1 and group 2 in the organism

phylogeny (Fig. 2A). In contrast to clade B strains, which clustered together in most *hrc*

phylogenies, strains from clades A and C were interspersed. This suggested numerous HGTs

between these two latter clades.

To characterize the gene flow affecting the T3SS cluster in *Xanthomonas* spp. strains,

potential recombinant sequences and their likely parental sequences were detected based on

phylogenetic incongruences (Martin et al., 2010). Identification of the likely origin of the

recombinant fragment can be achieved if at least one sequence resembling the donor

sequence is present in the data set. The identified exchanges concerned the entire sequence of

one or two adjacent genes in the concatenated *hrc* genes. The two genes for which the

number of exchanges were the highest were *hrpE* and *hrpB2* (32 and 26 events, respectively)

and the two genes for which the smallest number of exchange events were observed were

hrcC and *hrcT* (3 and 0 events, respectively). *X. arboricola* strains were the main recipients of recombination events (Fig. 3A). They mostly received genes from *X. dyei* and *X. hortorum* pv. *hederae*. Notably, most exchanges were detected within the recombinant network of *X. arboricola* and epidemic clones gave *hrp/hrc* alleles to strains belonging to this network, but no reverse events were detected. In contrast, only two *X. arboricola* strains were donors for other species (CFBP 1022 was donor for *X. cassavae* and CFBP 8149 for *X. hortorum*, *X. gardneri* and *X. cynarae*). T3SS gene exchanges were also detected between strains of the *X. axonopodis* species complex but remarkably no gene flow occurred between this clade and other clades.

For each individual T3SS coding gene, we estimated the evolutionary force responsible for observed polymorphism using the ρ/θ ratio. For most genes (14 out of 16) mutation had more impact than recombination on generating new alleles ($\rho/\theta < 1$) (Fig. 3B). Only two genes had a ρ/θ ratio above one, *hrcJ* ($\rho/\theta > 2$) and *hrcV* ($1 > \rho/\theta > 2$). In conclusion, within *hrc/hrp* genes, mutation was the major evolutionary force that have brought polymorphism and generated allelic variants at gene scale. This polymorphism was disseminated across the genus through homologous recombination of entire genes or contiguous genes.

T3E repertoires in *X. arboricola*

To decipher the diversity of T3E repertoires in *X. arboricola*, T3E coding genes were predicted for all genome sequences belonging to this species by a machine-learning approach dedicated to *Xanthomonas* organisms. Briefly, T3E encoding genes were searched for based on criteria referring to type three N-terminal secretion signal, structural disorder, regulation by HrpX/HrpG, GC content, codon usage, amino acid properties, and homology to known

and validated T3Es. Based on this prediction, a set of seven ancestral core T3E genes was observed. The predicted T3E repertoires were highly variable with some strains having no T3Es and others having up to 34 predicted T3Es (Fig. 4). Eight of the 14 strains lacking the T3SS cluster, were also deprived of T3E coding genes. In contrast, between one and two T3E genes (*avrBs2* and *xopR*) were identified in the remaining six strains (Data Set S3, Supporting information). While synteny in the *xopR* genomic environments has previously been shown (Merda et al., 2016), here we observed that genomic environments of *avrBs2* were also highly syntenic between all strains, with the exception of strains CFBP 7408 and CFBP 7409 (Fig. S4), favoring an ancestral acquisition and subsequent losses of these T3Es during *X. arboricola* evolution. The two strains of pathovar *guizotiae*, CFBP 7408 and CFBP 7409, probably lost and reacquired *avrBs2*. It has to be noted that *avrBs2* was systematically accompanied by three CDSs, namely *xylR*, a TonB-dependent receptor and a hypothetical protein that presented the same distribution in our collection whatever the genomic context (see Fig. S4). In addition to *xopR* and *avrBs2*, five other T3E genes (already described in *Xanthomonas* strains) were found in all *X. arboricola* strains having a T3SS. These five T3E genes were located within the T3SS cluster (Fig. 3B) and their distribution strictly followed the distribution of the T3SS cluster. However, among them were XopA, HpaA and HrpW, which while listed as T3Es in some studies (Hajri et al., 2009; Merda et al., 2016), are secreted regulator (HpaA) or harpin-like proteins and their effector function remains unclear (Lorenz et al., 2008; White et al., 2009). Synteny in the flanking regions of *avrBs2*, *xopR*, and of the five T3E genes associated with the T3SS cluster suggested that they were most probably acquired by an ancient *X. arboricola* strain, thus these seven T3E genes will be designated as the ancestral repertoire thereafter.

Pathogenic strains had a higher number of predicted T3E genes than commensal strains (Fig. 4). However, pathogenic strains CFBP 3122 and CFBP 3123 of pathovar *populi* lacked T3SS and T3E genes and hence represented an exception. Therefore the pathogenicity of these bacteria, previously qualified as opportunistic pathogens (Haworth & Spiers, 1992), may rely on different virulence factors. The T3E repertoire of pathogenic strains encompassed the ancestral repertoire and a large number of additional predicted T3E genes. Indeed, the pan-T3 effectome of *X. arboricola* was composed of 57 predicted T3Es and among them only 11 were found in both pathogenic and commensal strains, with the 46 others present exclusively in pathogenic strains. Most putative T3E genes identified in *X. arboricola* were already described in other *Xanthomonas* spp. This is the case for the seven T3E genes of the ancestral repertoire and 31 other T3E genes (Data Set S3, Supporting information). Among the 19 remaining T3E genes composing the pan-effectome, seven were known in other bacteria (*Ralstonia* and *Pseudomonas*) and 12 were putative novel T3E genes. Among these putative novel T3Es, six (T3E_14 to T3E_19) had a weak similarity (less than 30 % of sequence similarity) to T3E genes known in *Xanthomonas* (*xopAH*, *xopJ1*, *xopAO*, *xopAV*, *xopG*, and *xopM,* respectively) and thus are not considered as orthologous of these genes, but they could share a common ancestor.

The three successful pathovars (pvs. *pruni*, *corylina* and *juglandis*) shared ten T3E genes that were sequentially acquired in their common ancestor. These ten T3E genes were *xopX*, *xopV*, *xopL*, *xopK*, *xopN*, *xopAV*, *xopQ*, *avrXccA2*, *xopZ* and T3E_16 which shared 27.2% sequence similarity with *xopJ1*. To determine if their ancestral acquisition resulted from one or several events, we analyzed their genomic context. Contig alignment using CFBP 2528 as reference revealed that these T3E genes were dispersed along the chromosome, except *xopAV* and *xopQ* which were colocalized (Figs S5 and S6, Supporting information). The dispersal of these T3E genes along the genome sequences suggested that

they were acquired following several acquisition events. Given the synteny observed in the flanking regions of each of these T3E genes in the genomes of the successful pathovars (Fig. S5, Supporting information), it is likely that these independent acquisition events probably occurred in their ancestor before separation into three distinct pathovars.

Discussion

The acquisition and evolution of the T3SS have played major roles in ecological adaptation of pathogens, and HGT has been a driving force in T3SS evolutionary history at multiple evolutionary time scales. We investigated T3SS evolution in the *Xanthomonas* genus, a major clade of plant pathogens. Comparative genomic analyses of a collection of 82 strains allowed us to infer three ancestral acquisitions of the Hrp2 gene cluster during *Xanthomonas* evolution, two in group 2 strains and one in group 1 strains. Indeed, we highlighted an ancestral acquisition in the common ancestor of all group 2 species excluding *X. campestris*. This species, which diverged early in group 2, has a T3SS cluster at a different chromosomal location, supporting an independent acquisition event. The third ancestral T3SS acquisition occurred in group 1. A different genetic organization of the T3SS cluster, a high divergence among T3SS coding genes from the group 2 species, and the different genomic contexts of the T3SS clusters all indicate that group 1 strains probably acquired a different Hrp2 cluster independently as previously proposed by Jacobs et al. (2015). Before this study, *X. translucens* was the only group 1 species known to harbor a Hrp2 cluster (F. Wichmann et al., 2013). Our results indicate that this atypical Hrp2 cluster is shared with *X. theicola* and *X. hyacinthi* and that it was probably acquired by their common ancestor. T3SS cluster acquisitions occurred before speciation of most xanthomonads; capacity to interact with plants through translocation of T3Es would thus be an ancient trait of xanthomonads as it is

the case for other important plant bacterial pathogens (Diallo et al., 2012; Kirzinger et al., 2015).

After ancestral acquisition the T3SS was lost in some strains and species scattered throughout in the *Xanthomonas* phylogenetic tree (Fig.1). The scattering of strains without T3SS in the tree, the conservation of similar genomic environments in the T3SS positive strains, and a similar genome sequence in strains without T3SS are three lines of evidence in favor of the T3SS loss hypothesis. Absence of pseudogenes or remnants of T3SS encoding genes might be surprising, but a similar observation was made in nonpathogenic *P. syringae* strains, from which the entire cluster has been excised (Mohr et al., 2008). The loss hypothesis in commensal strains of *X. arboricola* species was previously proposed (Merda et al., 2016) based on Bayesian inference of gene gains and losses. Such complex scenarios with ancestral acquisition, losses and regains, have also been proposed in *Pantoea* genus (Kirzinger et al., 2015) and *P. syringae* (Clarke, Cai, Studholme, Guttman, & Vinatzer, 2010).

Losses of T3SS could be explained by a loss of function (Abby & Rocha, 2012). Indeed it could be beneficial to lose this energetically costly machinery if it does not enhance bacterial fitness (Gophna, Ron, & Graur, 2003). Thus, for commensal strains colonizing various plant hosts and with a limited set of T3Es (like *X. arboricola* group B strains) (Merda et al., 2016), the fitness cost provided by T3SS might be high and consequently it could be lost. T3SS-negative strains may also act as profiteers and benefit from the presence of T3SS-positive strains colonizing the same niche as demonstrated in murine infections by *Pseudomonas aeruginosa* (Czechowska, McKeithen-Mead, Al Moussawi, & Kazmierczak, 2014).

Once acquired, we showed that T3SS coding genes were prone to homologous recombination events leading to replacement of large fragments encompassing one complete gene, adjacent genes or even the entire cluster. The two genes for which the number of recombination events was the highest were *hrpE* and *hrpB2* which encode the Hrp pilin and the putative inner rod, respectively (Hartmann et al., 2012). These two proteins correspond to the early substrates of the secretion machinery. Weber and Koebnik (2006) observed positive diversifying selection in the *hrpE* sequence corresponding to the surface exposed part of the protein and interpreted it as an adaptative mechanism of the pathogen to escape recognition by the host. Homologous replacement of the *hrpE* gene by recombination could be an alternative mechanism to generate diversity and to escape host recognition. This latter mechanism has been extensively described in the mammalian pathogen *Neisseria gonorrhoeae* where it drives antigenic variation of the type IV pilus and avoidance of the host immune system (Obergfell & Seifert, 2015). The two genes that showed the fewest exchanges, *hrcC* and *hrcT*, encode highly conserved proteins located in the basal structure of the secretion system and embedded in the bacterial envelope. Within each gene, allelic polymorphism is mostly generated by mutation, except for *hrcJ* and *hrcV* (Fig. 3B). The study of genomic environment of the T3SS allowed us to distinguish two mechanisms of HGT: acquisition of a new cluster in a different chromosomal context as previously discussed, and homologous recombination within T3SS cluster. One homologous recombination event leading to entire T3SS cluster replacement was shown between *X. arboricola* pv. *guizotiae* and the phylogenetically distant strains CFBP 7912 and Nyagatare. Interestingly, all these strains originated from South-East Africa and were isolated from two crops (Niger seed and bean) used in mixed crop-livestock farming systems and as intercrops in maize production (Abera, Feyisa, & Friesen, 2009), making their co-occurrence plausible. Beside this single whole Hrp2 cluster replacement, numerous localized homologous

recombination events between strains of different species have perturbed the vertical inheritance signal. Similarly conflicts between phylogenies of some *hrp/hrc* genes and of housekeeping genes were observed in pseudomonads and enterobacterial plant pathogens (Sarris et al., 2013; Tegli, Gori, Cerboneschi, Cipriani, & Sisto, 2011) and a HGT event expanding through several *hrp* genes was previously suggested in pseudomonads (Sarris et al., 2013).

Understanding gene flow within and between populations sheds light on bacterial ecology. The study of "donor" and "recipient" strains of recombinant fragments showed that *X. arboricola* strains were the main "recipient", particularly in commensal strains, and *X. dyei* and *X. hortorum* were the two main donors (Fig. 3A). This suggests that commensal strains are found in sympatry with a large number of different *Xanthomonas* species because genetic material exchanges can only take place when individuals colonize the same niche. *X. dyei* and *X. arboricola* strains were isolated from the endemic species *Dysoxylum spectabile* in New-Zealand (Young, Wilkie, Park, & Watson, 2010). These observations reinforce the hypothesis proposed by Merda et al. (2016) that the commensal strains in *X. arboricola* are generalist organisms colonizing many different plants. In contrast, no gene flow at T3SS locus occurred between clade B strains and other clades. Divergent evolution of the T3SS cluster in this clade may have led to an optimized allelic combination. This result reinforces the major role of T3SS in this important clade of devastating host specialized pathogens within which the presence of theT3SS is conserved.

The function of T3SS is to deliver T3Es into host cells. In most strains devoid of T3SSs, no T3E genes could be detected in their genomes using machine learning approach and BLASTp (data not shown). Indeed, some T3E genes are housed in the T3SS cluster (Fig. 3B) and thus were lost with it. *xopR* and *avrBs2,* which are not located in T3SS cluster were found in the genomes of some commensal *Xanthomonas* strains lacking T3SS. Their

conserved genomic environments, when compared to strains with T3SSs, suggest that they are remnants of an ancestral T3E repertoire (Fig. S4, Supporting information) (Merda et al., 2016). A recent loss of the T3SS could explain why the T3Es were present despite the lack of theT3SS. Alternatively, *xopR* and *avrBs2* secretion might be mediated by the flagellum apparatus as demonstrated for some non-flagellar proteins (Journet, Hughes, & Cornelis, 2005). They might also have an additional function independent of the T3SS.

We have highlighted an extremely reduced ancestral core repertoire and stepwise acquisition of numerous additional T3Es in pathogenic strains of *X. arboricola*. Five of the seven core T3E genes were located in the T3SS cluster as previously observed in other *Xanthomonas* species (da Silva et al., 2002; Noel, Thieme, Nennstiel, & Bonas, 2002; Potnis et al., 2011; Teper et al., 2016). Among them, XopA, HpaA and HrpW should be better considered as accessory or translocation proteins that help the translocation process (Lorenz et al., 2008; Roux et al., 2015; White et al., 2009). Taking this into account, the *X. arboricola* core effectome comprises only four T3E genes (*xopF1*, *xopM*, *avrBs2* and *xopR*) and is comparable in size to that of *X. campestris* (Roux et al., 2015). Together, these results challenge the list of ten core T3E genes (*avrBs2, xopF1, xopK, xopL, xopN, xopP, xopQ, xopR, xopX, xopZ*) previously proposed (Ryan et al., 2011; White et al., 2009). *xopM*, missing in this list, was recently shown to be a T3E gene of *X. euvesicatoria* strain 85-10 (Schulze et al., 2012; Teper et al., 2016). Our BLASTp searches showed that it is present in most group 2 *Xanthomonas* species (data not shown). Considering that *xopR* and *avrBs2* were missing in only one and two strains, respectively, out of 13 *X. campestris* (Roux et al., 2015), we propose a list of four putative core *Xanthomonas* T3Es: AvrBs2, XopF1, XopM, and XopR. Interestingly, AvrBs2 contributes to bacterial fitness in field conditions, including epiphytic survival (G. Wichmann & Bergelson, 2004). It is required for full aggressiveness both in dicots and monocots and was shown to inhibit pathogen-associated molecular pattern-

triggered immune (PTI) responses in rice (S. Li et al., 2015; Zhao, Dahlbeck, Krasileva, Fong, & Staskawicz, 2011). Similarly, XopM inhibits immunity-associated cell death mediated by MAP kinase cascades (Teper, Sunitha, Martin, & Sessa, 2015) and XopR inhibits plant basal defenses (Akimoto-Tomiyama et al., 2012).

Besides the reduced ancestral core T3E repertoire, stepwise accumulation of additional T3Es has occurred in pathogenic strains and particularly in successful pathovars of *X. arboricola*. This accumulation appears to be a long-term evolutionary process as many T3Es were acquired before the radiation of the three successful pathovars. At the basal steps of pathogen emergence accumulation of numerous T3Es including *XopL, XopN, XopQ, XopX,* and *XopZ* occurred. These were shown to target PTI in addition to the ancestral T3Es, which are also involved in PTI suppression. This reinforces the idea that PTI suppression is crucial for pathogenic strains to achieve successful infection (Macho & Zipfel, 2015).

In conclusion, we showed three ancestral acquisitions of the Hrp2 cluster demonstrating that an intimate interaction with plants is an ancestral trait of xanthomonads. During radiation most species retained this ancestral T3SS but some lost it and subsequently it was re-acquired in some strains. Mutation is the main evolutionary force generating new *hrc/hrp* alleles. In group 2 *Xanthomonas*, the inter- and intra-species homologous recombination of large fragments expanding through one or more genes shuffles this polymorphism generating new allelic combinations in Hrp2 clusters. A set of four ancestral core T3E genes is found in commensal strains and pathogens in *X. arboricola* that may approximate the *Xanthomonas* ancestral core effectome. We propose that these may allow the strains to overcome basal plant immunity under specific environmental conditions, but could have a fitness cost explaining why they were lost in some strains. In contrast, some strains experienced a different evolutionary pathway with stepwise accumulation of T3Es that probably accounts for their efficacy to overcome plant immunity and could explain the high

aggressiveness. *X. arboricola* represents the archetype of this evolutionary scenario, which seems to share similarities with the one proposed for *P. syringae* (Lindeberg et al., 2012) and culminates in a narrow host-range.

Acknowledgments

References

Abby, S. S., & Rocha, E. P. C. (2012). The non-flagellar type III secretion system evolved from the bacterial flagellum and diversified into host-cell adapted systems. *Plos Genetics, 8*(9). doi: 10.1371/journal.pgen.1002983

Abera, T., Feyisa, D., & Friesen, D. K. (2009). Effects of Crop Rotation and N-P Fertilizer Rate on Grain Yield and Related Characteristics of Maize and Soil Fertility at Bako, Western Oromia, Ethiopia. *East African Journal of Sciences, 3*(1), 70-79.

Akimoto-Tomiyama, C., Furutani, A., Tsuge, S., Washington, E. J., Nishizawa, Y., Minami, E., & Ochiai, H. (2012). XopR, a type III effector secreted by *Xanthomonas oryzae* pv. *oryzae*, suppresses microbe-associated molecular pattern-triggered immunity in *Arabidopsis thaliana*. *Molecular Plant-Microbe Interactions, 25*(4), 505-514. doi: 10.1094/MPMI-06-11-0167

Barret, M., Egan, F., Moynihan, J., Morrissey, J. P., Lesouhaitier, O., & O'Gara, F. (2013). Characterization of the SPI-1 and Rsp type three secretion systems in *Pseudomonas fluorescens* F113. *Environmental Microbiology Reports, 5*(3), 377-386. doi: 10.1111/1758-2229.12039

Carrere, S., Cottret, L., Rancurel, C., & Briand, M. (2015). Orthomcl-Companion: a user friendly tool to analyze protein families [version 1; not peer reviewed]. *F1000Research, 4*, 489. doi: 10.7490/f1000research.1110226.1

Carver, T., Thomson, N., Bleasby, A., Berriman, M., & Parkhill, J. (2009). DNAPlotter: circular and linear interactive genome visualization. *Bioinformatics, 25*(1), 119-120. doi: 10.1093/bioinformatics/btn578

Cesbron, S., Briand, M., Essakhi, S., Gironde, S., Boureau, T., Manceau, C., . . . Jacques, M.-A. (2015). Comparative genomics of pathogenic and nonpathogenic strains of *Xanthomonas arboricola* unveil molecular and evolutionary events linked to pathoadaptation. *Frontiers in Plant Science, 6*. doi: 10.3389/fpls.2015.01126

Clarke, C. R., Cai, R. M., Studholme, D. J., Guttman, D. S., & Vinatzer, B. A. (2010). *Pseudomonas syringae* Strains Naturally Lacking the Classical *P. syringae hrp/hrc* Locus Are Common Leaf Colonizers Equipped with an Atypical Type III Secretion System. *Molecular Plant-Microbe Interactions, 23*(2), 198-210. doi: 10.1094/mpmi-23-2-0198

Czechowska, K., McKeithen-Mead, S., Al Moussawi, K., & Kazmierczak, B. I. (2014). Cheating by type 3 secretion system-negative Pseudomonas aeruginosa during pulmonary infection. *Proceedings of the National Academy of Sciences, 111*(21), 7801-7806. doi: 10.1073/pnas.1400782111

da Silva, A. C., Ferro, J. A., Reinach, F. C., Farah, C. S., Furlan, L. R., Quaggio, R. B., . . . Kitajima, J. P. (2002). Comparison of the genomes of two *Xanthomonas* pathogens with differing host specificities. *Nature, 417*, 459-463. doi: 10.1038/417459a

Darling, A. C., Mau, B., Blattner, F. R., & Perna, N. T. (2004). Mauve: multiple alignment of conserved genomic sequence with rearrangements. *Genome Research, 14*(7), 1394-1403. doi: 10.1101/gr.2289704

Diallo, M. D., Monteil, C. L., Vinatzer, B. A., Clarke, C. R., Glaux, C., Guilbaud, C., . . . Morris, C. E. (2012). *Pseudomonas syringae* naturally lacking the canonical type III secretion system are ubiquitous in nonagricultural habitats, are phylogenetically diverse and can be pathogenic. *The ISME Journal, 6*(7), 1325-1335. doi: 10.1038/ismej.2011.202

Diepold, A., & Armitage, J. P. (2015). Type III secretion systems: the bacterial flagellum and the injectisome. *Philosophical Transactions of the Royal Society B: Biological Sciences, 370*(1679). doi: 10.1098/rstb.2015.0020

Edgar, R. C. (2004). MUSCLE: multiple sequence alignment with high accuracy and high throughput. *Nucleic Acids Research, 32*(5), 1792-1797. doi: 10.1093/nar/gkh340

Gophna, U., Ron, E. Z., & Graur, D. (2003). Bacterial type III secretion systems are ancient and evolved by multiple horizontal-transfer events. *Gene, 312*, 151-163. doi: 10.1016/S0378-1119(03)00612-7

Guy, L., Roat Kultima, J., & Andersson, S. G. E. (2010). genoPlotR: comparative gene and genome visualization in R. *Bioinformatics, 26*(18), 2334-2335. doi: 10.1093/bioinformatics/btq413

Hajri, A., Brin, C., Hunault, G., Lardeux, F., Lemaire, C., Manceau, C., . . . Poussier, S. (2009). A "Repertoire for Repertoire" Hypothesis: Repertoires of Type Three Effectors are Candidate Determinants of Host Specificity *Xanthomonas*. *PLoS ONE, 4*(8). doi: 10.1371/journal.pone.0006632

Hartmann, N., Schulz, S., Lorenz, C., Fraas, S., Hause, G., & Büttner, D. (2012). Characterization of HrpB2 from *Xanthomonas campestris* pv. *vesicatoria* identifies protein regions that are essential for type III secretion pilus formation. Microbiology, 158(5), 1334-1349. doi: doi:10.1099/mic.0.057604-0

Haworth, R. H., & Spiers, A. G. (1992). Isolation of *Xanthomonas campestris* pv. *populi* from stem lesions on *Salix matsudana* X *alba* 'Aokautere' in New Zealand. *European Journal of Forest Pathology, 22*(4), 247-251. doi: 10.1111/j.1439-0329.1992.tb00789.x

Jacobs, J. M., Pesce, C., Lefeuvre, P., & Koebnik, R. (2015). Comparative genomics of a cannabis pathogen reveals insight into the evolution of pathogenicity in *Xanthomonas*. *Frontiers in Plant Science, 6*(431). doi: 10.3389/fpls.2015.00431

Journet, L., Hughes, K. T., & Cornelis, G. R. (2005). Type III secretion: a secretory pathway serving both motility and virulence (Review). *Molecular Membrane Biology, 22*(1-2), 41-50. doi: 10.1080/09687860500041858

Kearse, M., Moir, R., Wilson, A., Stones-Havas, S., Cheung, M., Sturrock, S., . . . Drummond, A. (2012). Geneious Basic: an integrated and extendable desktop software platform for the organization and analysis of sequence data. *Bioinformatics, 28*(12), 1647-1649. doi: 10.1093/bioinformatics/bts199

Kirzinger, M. W., Butz, C. J., & Stavrinides, J. (2015). Inheritance of *Pantoea* type III secretion systems through both vertical and horizontal transfer. *Molecular Genetics and Genomics, 290*(6), 2075-2088. doi: 10.1007/s00438-015-1062-2

Krzywinski, M., Schein, J., Birol, I., Connors, J., Gascoyne, R., Horsman, D., . . . Marra, M. A. (2009). Circos: an information aesthetic for comparative genomics. *Genome Research, 19*(9), 1639-1645. doi: 10.1101/gr.092759.109

Li, L., Stoeckert, C. J., Jr., & Roos, D. S. (2003). OrthoMCL: identification of ortholog groups for eukaryotic genomes. *Genome Research, 13*(9), 2178-2189. doi: 10.1101/gr.1224503

Li, R., Zhu, H., Ruan, J., Qian, W., Fang, X., Shi, Z., . . . Wang, J. (2010). De novo assembly of human genomes with massively parallel short read sequencing. *Genome Research, 20*(2), 265-272. doi: 10.1101/gr.097261.109

Li, S., Wang, Y., Wang, S., Fang, A., Wang, J., Liu, L., . . . Sun, W. (2015). The Type III Effector AvrBs2 in *Xanthomonas oryzae* pv. *oryzicola* Suppresses Rice Immunity and Promotes Disease Development. *Molecular Plant-Microbe Interactions, 28*(8), 869-880. doi: 10.1094/mpmi-10-14-0314-r

Lindeberg, M., Cunnac, S., & Collmer, A. (2012). *Pseudomonas syringae* type III effector repertoires: last words in endless arguments. *Trends in Microbiology, 20*(4), 199-208. doi: 10.1016/j.tim.2012.01.003

Lorenz, C., Kirchner, O., Egler, M., Stuttmann, J., Bonas, U., & Büttner, D. (2008). HpaA from *Xanthomonas* is a regulator of type III secretion. *Molecular Microbiology, 69*(2), 344-360. doi: 10.1111/j.1365-2958.2008.06280.x

Lower, M., & Schneider, G. (2009). Prediction of Type III Secretion Signals in Genomes of Gram-Negative Bacteria. *PLoS ONE, 4*(6). doi: 10.1371/journal.pone.0005917

Macho, A. P., & Zipfel, C. (2015). Targeting of plant pattern recognition receptor-triggered immunity by bacterial type-III secretion system effectors. *Current Opinion in Microbiology, 23*, 14-22. doi: 10.1016/j.mib.2014.10.009

Marguerettaz, M., Pieretti, I., Gayral, P., Puig, J., Brin, C., Cociancich, S., . . . Royer, M. (2011). Genomic and evolutionary features of the SPI-1 type III secretion

system that is present in *Xanthomonas albilineans* but is not essential for xylem colonization and symptom development of sugarcane leaf scald. *Molecular Plant-Microbe Interactions, 24*(2), 246-259. doi: 10.1094/MPMI-08-10-0188

Martin, D. P., Lemey, P., Lott, M., Moulton, V., Posada, D., & Lefeuvre, P. (2010). RDP3: a flexible and fast computer program for analyzing recombination. *Bioinformatics, 26*(19), 2462-2463. doi: 10.1093/bioinformatics/btq467

McCann, H. C., & Guttman, D. S. (2008). Evolution of the type III secretion system and its effectors in plant-microbe interactions. *New Phytologist, 177*(1), 33-47. doi: 10.1111/j.1469-8137.2007.02293.x

McDermott, J. E., Corrigan, A., Peterson, E., Oehmen, C., Niemann, G., Cambronne, E. D., . . . Heffron, F. (2011). Computational Prediction of Type III and IV Secreted Effectors in Gram-Negative Bacteria. *Infection and Immunity, 79*(1), 23-32. doi: 10.1128/iai.00537-10

Merda, D., Bonneau, S., Guimbaud, J.-F., Durand, K., Brin, C., Boureau, T., . . . Fischer-Le Saux, M. (2016). Recombination-prone bacterial strains form a reservoir from which epidemic clones emerge in agroecosystems. *Environmental Microbiology Reports, 8*, 572-581. doi: 10.1111/1758-2229.12397

Mohr, T. J., Liu, H., Yan, S., Morris, C. E., Castillo, J. A., Jelenska, J., & Vinatzer, B. A. (2008). Naturally occurring nonpathogenic isolates of the plant pathogen *Pseudomonas syringae* lack a type III secretion system and effector gene orthologues. *Journal of Bacteriology, 190*(8), 2858-2870. doi: 10.1128/jb.01757-07

Naushad, H. S., & Gupta, R. S. (2013). Phylogenomics and Molecular Signatures for Species from the Plant Pathogen-Containing Order Xanthomonadales. *PLoS ONE, 8*(2). doi: 10.1371/journal.pone.0055216

Noel, L., Thieme, F., Nennstiel, D., & Bonas, U. (2002). Two novel type III-secreted proteins of *Xanthomonas campestris* pv. *vesicatoria* are encoded within the *hrp* pathogenicity island. *Journal of Bacteriology, 184*(5), 1340-1348. doi: 10.1128/JB.184.5.1340–1348.2002

Obergfell, K. P., & Seifert, H. S. (2015). Mobile DNA in the Pathogenic *Neisseria*. *Microbiology Spectrum*, 3(1). doi: doi:10.1128/microbiolspec.MDNA3-0015-2014

Pieretti, I., Cociancich, S., Bolot, S., Carrere, S., Morisset, A., Rott, P., & Royer, M. (2015). Full Genome Sequence Analysis of Two Isolates Reveals a Novel *Xanthomonas* Species Close to the Sugarcane Pathogen *Xanthomonas albilineans*. *Genes, 6*(3), 714-733. doi: 10.3390/genes6030714

Posada, D. (2008). jModelTest: Phylogenetic Model Averaging. *Molecular Biology and Evolution, 25*(7), 1253-1256. doi: 10.1093/molbev/msn083

Potnis, N., Krasileva, K., Chow, V., Almeida, N. F., Patil, P. B., Ryan, R. P., . . . Jones, J. B. (2011). Comparative genomics reveals diversity among xanthomonads infecting tomato and pepper. *BMC Genomics, 12*. doi: 10.1186/1471-2164-12-146

Ranwez, V., Harispe, S., Delsuc, F., & Douzery, E. J. (2011). MACSE: Multiple Alignment of Coding SEquences accounting for frameshifts and stop codons. *PLoS ONE, 6*(9). doi: 10.1371/journal.pone.0022594

Rodriguez, R. L., Grajales, A., Arrieta-Ortiz, M. L., Salazar, C., Restrepo, S., & Bernal, A. (2012). Genomes-based phylogeny of the genus *Xanthomonas*. *BMC Microbiology, 12*(43), 1471-2180. doi: 10.1186/12-43

Roux, B., Bolot, S., Guy, E., Denance, N., Lautier, M., Jardinaud, M.-F., . . . Noel, L. D. (2015). Genomics and transcriptomics of *Xanthomonas campestris* species challenge the concept of core type III effectome. *BMC Genomics, 16*. doi: 10.1186/s12864-015-2190-0

Ryan, R. P., Vorholter, F. J., Potnis, N., Jones, J. B., Van Sluys, M. A., Bogdanove, A. J., & Dow, J. M. (2011). Pathogenomics of *Xanthomonas*: understanding bacterium-plant interactions. *Nature Reviews Microbiology, 9*(5), 344-355. doi: 10.1038/nrmicro2558

Sallet, E., Gouzy, J., & Schiex, T. (2014). EuGene-PP: a next-generation automated annotation pipeline for prokaryotic genomes. *Bioinformatics, 30*(18), 2659-2661. doi: 10.1093/bioinformatics/btu366

Sarkar, S. F., Gordon, J. S., Martin, G. B., & Guttman, D. S. (2006). Comparative genomics of host-specific virulence in *Pseudomonas syringae*. *Genetics, 174*(2), 1041-1056. doi: 10.1534/genetics.106.060996

Sarris, P. F., Trantas, E. A., Baltrus, D. A., Bull, C. T., Wechter, W. P., Yan, S., . . . Goumas, D. E. (2013). Comparative Genomics of Multiple Strains of *Pseudomonas cannabina* pv. *alisalensis*, a Potential Model Pathogen of Both Monocots and Dicots. *PLoS ONE, 8*(3). doi: 10.1371/journal.pone.0059366

Schliep, K. P. (2011). phangorn: phylogenetic analysis in R. *Bioinformatics, 27*(4), 592-593. doi: 10.1093/bioinformatics/btq706

Schulze, S., Kay, S., Büttner, D., Egler, M., Eschen-Lippold, L., Hause, G., . . . Bonas, U. (2012). Analysis of new type III effectors from *Xanthomonas* uncovers XopB and XopS as suppressors of plant immunity. *New Phytologist, 195*(4), 894-911. doi: 10.1111/j.1469-8137.2012.04210.x

Shimodaira, H., & Hasegawa, M. (1999). Multiple comparisons of log-likelihoods with applications to phylogenetic inference. *Molecular Biology and Evolution, 16*(8), 1114-1116.

Studholme, D. J., Wasukira, A., Paszkiewicz, K., Aritua, V., Thwaites, R., Smith, J., & Grant, M. (2011). Draft Genome Sequences of *Xanthomonas sacchari* and Two Banana-Associated Xanthomonads Reveal Insights into the *Xanthomonas* Group 1 Clade. *Genes, 2*(4), 1050-1065. doi: 10.3390/genes2041050

Tampakaki, A. P., Skandalis, N., Gazi, A. D., Bastaki, M. N., Sarris, P. F., Charova, S. N., . . . Panopoulos, N. J. (2010). Playing the "Harp": evolution of our understanding of hrp/hrc genes. *Annual Review of Phytopathology, 48*(1), 347-370. doi: 10.1146/annurev-phyto-073009-114407

Tegli, S., Gori, A., Cerboneschi, M., Cipriani, M. G., & Sisto, A. (2011). Type Three Secretion System in *Pseudomonas savastanoi* Pathovars: Does Timing Matter? *Genes, 2*(4), 957-979. doi: 10.3390/genes2040957

Teper, D., Burstein, D., Salomon, D., Gershovitz, M., Pupko, T., & Sessa, G. (2016). Identification of novel *Xanthomonas euvesicatoria* type III effector proteins by a machine-learning approach. *Molecular Plant Pathology, 17*(3), 398-411. doi: 10.1111/mpp.12288

Teper, D., Sunitha, S., Martin, G. B., & Sessa, G. (2015). Five Xanthomonas type III effectors suppress cell death induced by components of immunity-associated MAP kinase cascades. *Plant Signaling & Behavior, 10*(10). doi: 10.1080/15592324.2015.1064573

Triplett, L. R., Verdier, V., Campillo, T., Van Malderghem, C., Cleenwerck, I., Maes, M., . . . Leach, J. E. (2015). Characterization of a novel clade of *Xanthomonas* isolated from rice leaves in Mali and proposal of *Xanthomonas maliensis* sp nov. *Antonie Van Leeuwenhoek International Journal of General and Molecular Microbiology, 107*(4), 869-881. doi: 10.1007/s10482-015-0379-5

Troisfontaines, P., & Cornelis, G. R. (2005). Type III secretion: more systems than you think. *Physiology, 20*, 326-339. doi: 10.1152/physiol.00011.2005

Weber, E., & Koebnik, R. (2006). Positive Selection of the Hrp Pilin HrpE of the Plant Pathogen *Xanthomonas*. *Journal of Bacteriology*, 188(4), 1405-1410. doi: 10.1128/jb.188.4.1405-1410.2006

White, F. F., Potnis, N., Jones, J. B., & Koebnik, R. (2009). The type III effectors of *Xanthomonas*. *Molecular Plant Pathology, 10*(6), 749-766. doi: 10.1111/j.1364-3703.2009.00590.x

Wichmann, F., Vorhölter, F.-J., Hersemann, L., Widmer, F., Blom, J., Niehaus, K., . . . Kölliker, R. (2013). The noncanonical type III secretion system of

Xanthomonas translucens pv. *graminis* is essential for forage grass infection. *Molecular Plant Pathology, 14*(6), 576-588. doi: 10.1111/mpp.12030

Wichmann, G., & Bergelson, J. (2004). Effector genes of *Xanthamonas axonopodis* pv. *vesicatoria* promote transmission and enhance other fitness traits in the field. *Genetics, 166*(2), 693-706. doi: 10.1534/genetics.166.2.693

Young, J. M., Park, D. C., Shearman, H. M., & Fargier, E. (2008). A multilocus sequence analysis of the genus *Xanthomonas*. *Systematic and Applied Microbiology, 31*(5), 366-377. doi: 10.1016/j.syapm.2008.06.004

Young, J. M., Wilkie, J. P., Park, D. C., & Watson, D. R. W. (2010). New Zealand strains of plant pathogenic bacteria classified by multi-locus sequence analysis; proposal of *Xanthomonas dyei* sp. nov. *Plant Pathology, 59*(2), 270-281. doi: 10.1111/j.1365-3059.2009.02210.x

Zerbino, D. R., & Birney, E. (2008). Velvet: algorithms for *de novo* short read assembly using de Bruijn graphs. *Genome Research, 18*(5), 821-829. doi: 10.1101/gr.074492.107

Zhao, B., Dahlbeck, D., Krasileva, K. V., Fong, R. W., & Staskawicz, B. J. (2011). Computational and Biochemical Analysis of the *Xanthomonas* Effector AvrBs2 and Its Role in the Modulation of *Xanthomonas* Type Three Effector Delivery. *Plos Pathogens, 7*(12). doi: 10.1371/journal.ppat.1002408

Data accessibility

The whole genome sequences obtained for this project have been deposited in Genblank. Accession numbers are available in Data Set S1 (Supporting information). Most bacterial strains used in this study are available at the microbial resource center CIRM-CFBP (Beaucouzé, INRA, France; http://www6.inra.fr/cirm_eng/CFBP-Plant-Associated-Bacteria)

Author Contributions

Figure Legends

Fig. 1 Maximum likelihood phylogeny based on the concatenated sequences of the core proteome (993 proteins) of 80 strains representing the entire *Xanthomonas* genus and schematic representation of T3SS genomic environments. The T3SS cluster is represented by the letters HRP, its genomic environments (20 kb on each side) by coloured rectangles and its genomic contexts (200 Kb on each side) by hatched rectangles in the right column. Different colours correspond to different genomic environments or contexts (Fig. S1 and S2, Supporting information). The colour of the letters HRP represents the different cluster organisations; HRP written in red represents the cluster organisation found in group 2 xanthomonads and HRP written in green represents the one found in group 1. Dotted line represents absence of information due to contig interruption. In Hrp-negative strains, HRP letters are replaced by the number of CDS found in place of T3SS cluster at the putative T3SS cluster insertion site. Genomic environments of the insertion site are represented as described above. . Probable T3SS acquisition events are represented by red arrow, loss events by blue arrow, and genomic rearrangements by green circled arrow. A dotted arrow represents hypothesis of T3SS loss and re-acquisition. Bootstrap scores (100 bootstraps) higher than 85% are displayed at each node.

Fig. 2 Comparison of organism and T3SS phylogenies and schematic representation of T3SS genomic environments. These two phylogenies were constructed in maximum likelihood. (A) The organism phylogeny is based on the concatenated sequences of the core proteome (1135 proteins) of 61 *Xanthomonas* spp. strains harboring a T3SS cluster. (B) The T3SS phylogeny is based on the concatenated sequences of 10 *hrc* genes. For strains belonging to *X. arboricola* a colour code was used to represent the three genetic groups previously defined (Merda et al., 2016). Group A strains are indicated in red, group B strains in green, and group C strains in blue. Strains of all other species of *Xanthomonas* are indicated in black. Bootstrap scores (100 bootstraps) higher than 85% are displayed at each node. T3SS clusters and their genomic environments (20 kb on each side of T3SS cluster) are represented as explained in the legend of Fig. 1.

Fig. 3 Gene flow affecting the T3SS cluster. (A) Representation of recombination events affecting 16 *hrc*/*hrp* genes of the T3SS cluster in *Xanthomonas* genus. The donor and recipient strains were identified with RDP software, and the representation was obtained using Circos. Each strain is represented by a rectangle of a different colour. The recombination events are represented by a link between donor and recipient strains. The colour of the link corresponds to the colour of the donor and indicates the direction of recombination event. The width of the links represents the number of genes involved in the recombination events. For strains belonging to *X. arboricola* a colour code was used to represent the three groups previously defined (Merda et al., 2016). Group A strains are indicated in red, group B strains in green, and group C strains in blue. (B) Representation of

ratios of recombination rate vs mutation rate (ρ/θ) along the T3SS cluster using 61 genomes representing the genus diversity. Ratios were calculated for the 16 *hrc/hrp* genes of the core region of T3SS cluster using RDP software. Arrows are shaded according to the shading scale which indicates the range of the ρ/θ value. The black arrows represent *hpa* and T3E genes for which ρ/θ was not calculated. Genetic organization of the cluster is based on the sequence of CFBP 2528. In red are represented the five core T3E genes located in the T3SS cluster of *X. arboricola* strains.

Fig. 4 Representation of T3E repertoires in *X. arboricola* strains. The phylogeny was performed in maximum likelihood using the concatenated sequences of 1,705 CDS composing the core genome of these 44 strains. Bootstrap values (100 bootstraps) higher than 85% are indicated at each node. Pathogenic strains are represented in red and commensal ones in blue. At the tip of each branch the orange triangles represent the presence of T3SS cluster and bars represent the composition of the T3E repertoire according to the legend.

Supporting information

Additional supporting information may be found in the online version of this article.

Fig. S1 Comparisons of genomic environments of T3SS clusters in different *Xanthomonas* species. Genomic environments (20 kb on each side) were compared using the R package GenoplotR. The genes of the T3SS cluster are represented by red arrows. Pink arrows represent genes encoding transposases, orange arrows represent integrons, grey arrows represent phages. Other genes are represented by blue arrows. DNA fragments showing BLASTn similarities are connected with grey shading. (A) Comparison of strains representing all the phylogenetic clusters identified in the *Xanthomonas* genus. Strains are ordered according to their phylogenetic relationships. (B) to (F) : examples of comparisons showing similarities and differences between genomic environments of T3SS cluster. Similar genomic environments of the T3SS cluster were highlighted by bars of the same colour placed above the schematic representation of the sequences. (B) Comparison between the strain CFBP 7179 of *X. arboricola* used as reference (representing the genomic environment retrieved in *X. arboricola* strains), *X. bromi* (CFBP 1976) and *X. oryzae* (BAI3). This comparison reveals that the genomic environment of *X. bromi* T3SS cluster shares similarities with the one of *X. arboricola* but not with the one of *X. oryzae* (this latter is shared by other clade B species). (C). Comparisons showing the diversity of genomic environments of T3SS cluster in *X. codiaei*, "*X. cannabis*", *X. cassavae*, and *X. dyei* and absence of similarities (except for *X. dyei*) with the genomic environment of clade B represented in green. (D). Comparisons showing the mosaic structure of the genomic environment of T3SS cluster in *X. arboricola* pv. *guizotiae* and in *X. dyei*. (E). Comparison showing that the genomic environment of T3SS cluster in the group 1 species *X. translucens* shares no similarity with the one retrieved in group 2 species from clades A and B. (F).

Comparison showing similarities between the genomic environments of T3SS cluster in the three group 1 species *X. translucens*, *X. hyacinthi* and *X. theicola*.

Fig. S2 Comparisons of large genomic environments of the T3SS clusters in different *Xanthomonas* species using a window of 200 kb upstream and downstream of the cluster. Genomic environments were compared using the R package GenoplotR. The genes of the T3SS cluster are represented in red; other genes are represented in blue. DNA fragments showing similarities are connected with grey shading.

Fig. S3 Individual maximum likelihood phylogenies built for each *hrc/hrp* gene coding for the T3SS. Bootstrap scores (1000 bootstraps) higher than 85% are displayed at each node.

Fig. S4 Genomic environments of *avrBs2* in *Xanthomonas arboricola* strains. On the left, the dendrogram corresponds to the phylogenetic relationship between strains inferred from the core genome. On the right, genomic environments of *avrBs2* insertion site, within a window of 20 kb upstream and downstream of *avrBs2*. Red arrows represent *avrBs2*. Pink arrows represent genes encoding transposases. Blue arrows represent other genes within genomic environments. DNA fragments sharing similarities are connected with gray shading.

Fig. S5 Genomic environments of 10 predicted type three effector (T3E) genes specific to *Xanthomonas arboricola* group A strains. On the left, the dendrogram corresponds to the phylogenetic relationship between strains. On the right, genomic environments of predicted T3E genes, within a window of 20 kb upstream and downstream of the gene, are represented. Red arrows represent predicted T3E genes. Pink arrows represent genes encoding transposases. Green arrows represent phages. Blue arrows represent other genes within genomic environments. DNA fragments sharing similarities are connected with gray shading.

Fig. S6 Graphical circular representation of the draft genomes of *Xanthomonas arboricola* strains belonging to the three successful pathovars : pv. *juglandis* (CFBP 2528, CFBP 7179, CFBP 8253), pv. *pruni* (CFBP 3894) and pv. *corylina* (CFBP 2565, CFBP 1159). The contigs were ordered by Mauve using the CFBP 2528 genome sequence as reference. Blue arrows represent the core T3E genes, red arrows represent the 10 TE3 genes acquired by the common ancestor of these strains, and pink arrows represent the T3E genes independently acquired by the strains. Black arrows represent the T3SS coding genes.

Data set S1 Whole genome sequences used in this study

Data set S2 T3SS coding genes used as query in BLAST searches

Data set S3 Repertoires of predicted T3E genes in *Xanthomonas arboricola*

Table S1 Results of Shimodaira-Hasegawa tests comparing phylogenies of T3SS coding genes in *Xanthomonas*
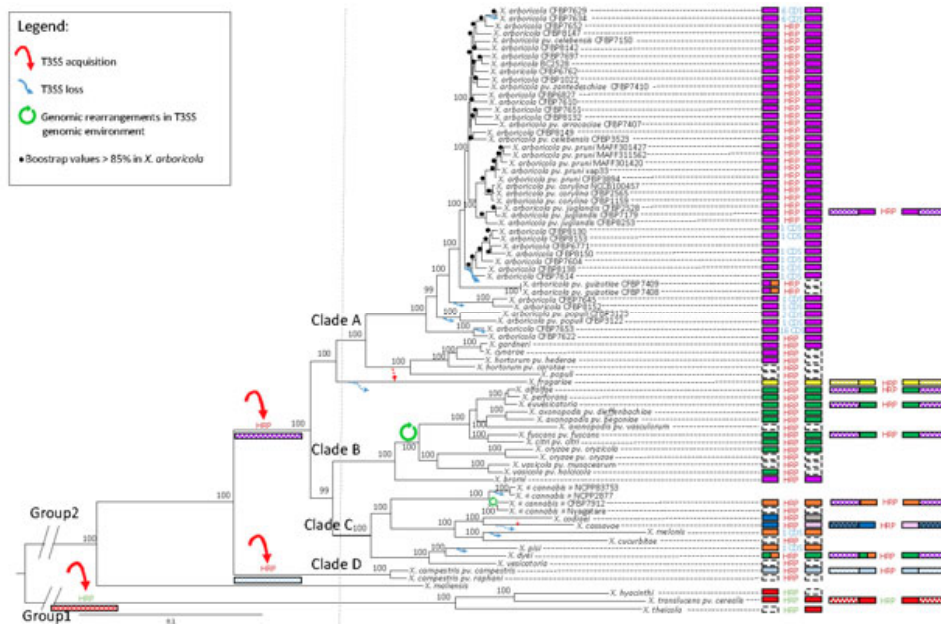

FIG 1 Maximum likelihood phylogeny based on the concatenated sequences of the core proteome (993 proteins) of 80 strains representing the entire *Xanthomonas* genus and schematic representation of T3SS genomic environments. The T3SS cluster is represented by the letters HRP, its genomic environments (20 kb on each side) by coloured rectangles and its genomic contexts (200 Kb on side) by hatched rectangles in the right column. Different colours correspond to different genomic environments or contexts (Fig. S1 and S2, Supporting information). The colour of the letters HRP represents the different cluster organisations, HRP written in red represents the cluster organisation found in group 2 xanthomonads and HRP written in green represents the one found in group 1. Dotted line represents absence of information due to contig interruption. In Hrp-negative strains, HRP letters are replaced by the number of CDS found in place of T3SS cluster at the putative T3SS cluster insertion site. Genomic environments of the insertion site are represented as described above. Probable T3SS acquisition events are represented by red arrow, loss events by blue arrow, and genomic rearrangements by green circled arrow. A dotted arrow represents hypothesis of T3SS loss and re-acquisition. Bootstrap scores (100 bootstraps) higher than 85% are displayed at each node.
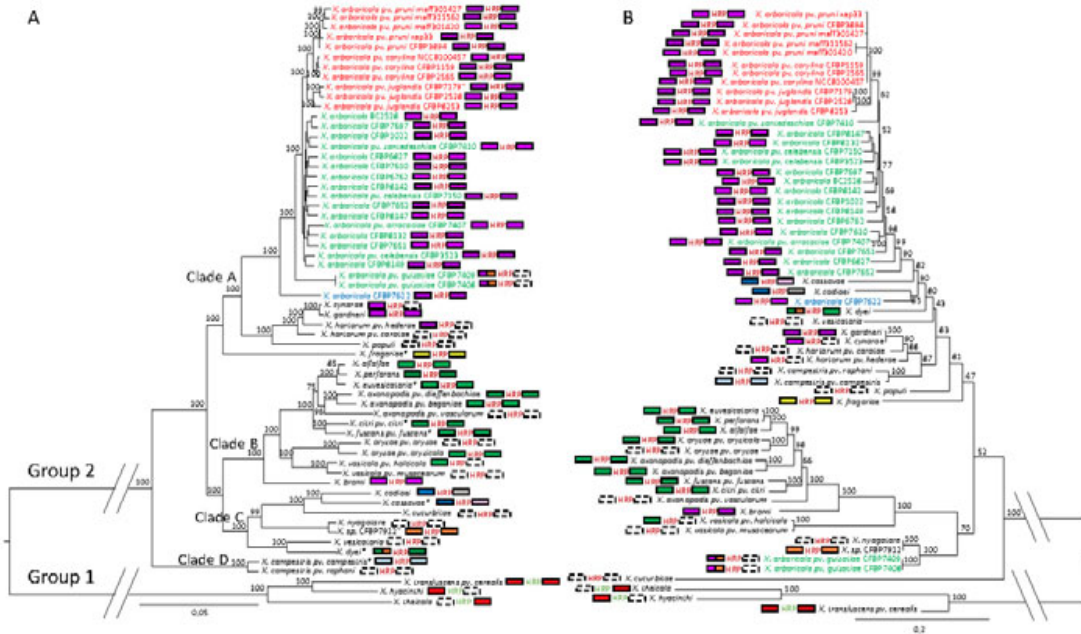
Fig. 2 Comparison of organism and T3SS phylogenies and schematic representation of T3SS genomic environments. These two phylogenies were constructed in maximum likelihood. (A) The organism phylogeny is based on the concatenated sequences of the core proteome (1135 proteins) of 61 *Xanthomonas* spp. strains harboring a T3SS cluster. (B) The T3SS phylogeny is based on the concatenated sequences of 10 *hrc* genes. For strains belonging to *X. arboricola* a color code was used to represent the three genetic groups previously defined (Merda et al., 2016). Group A strains are indicated in red, group B strains in green, and group C strains in blue. Strains of all other species of *Xanthomonas* are indicated in black. Bootstrap scores (100 bootstraps) higher than 85% are displayed at each node. T3SS clusters and their genomic environments (20 kb on each side of T3SS cluster) are represented as explained in the legend of Fig. 1.
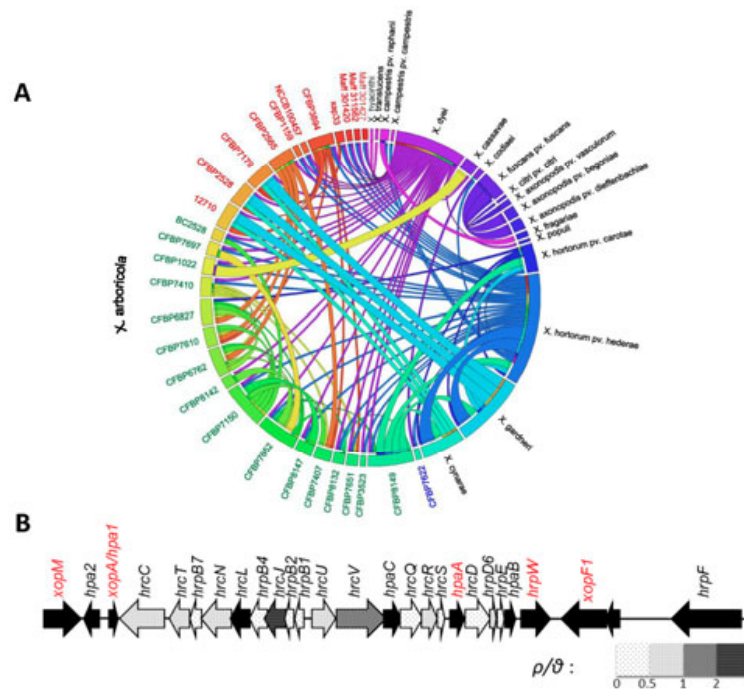
Fig. 3 Gene flow affecting the T3SS cluster. (A) Representation of recombination events affecting 16 *hrc/hrp* genes of the T3SS cluster in *Xanthomonas* genus. The donor and recipient strains were identified with RDP software, and the representation was obtained using Circos. Each strain is represented by a rectangle of a different color. The recombination events are represented by a link between donor and recipient strains. The color of the link corresponds to the color of the donor and indicates the direction of recombination event. The width of the links represents the number of genes involved in the recombination events. For strains belonging to *X. arboricola* a color code was used to represent the three groups previously defined (Merda et al., 2016). Group A strains are indicated in red, group B strains in green, and group C strains in blue. (B) Representation of ratios of recombination rate vs mutation rate (ρ/θ) along the T3SS cluster using 61 genomes representing the genus diversity. Ratios were calculated for the 16 *hrc/hrp* genes of the core region of T3SS cluster using RDP software. Arrows are shaded according to the shading scale which indicates the range of the ρ/θ value. The black arrows represent *hpa* and T3E genes for which ρ/θ was not calculated. Genetic organization of the cluster is based on the sequence of CFBP 2528. In red are represented the five core T3E genes located in the T3SS cluster of *X. arboricola* strains.
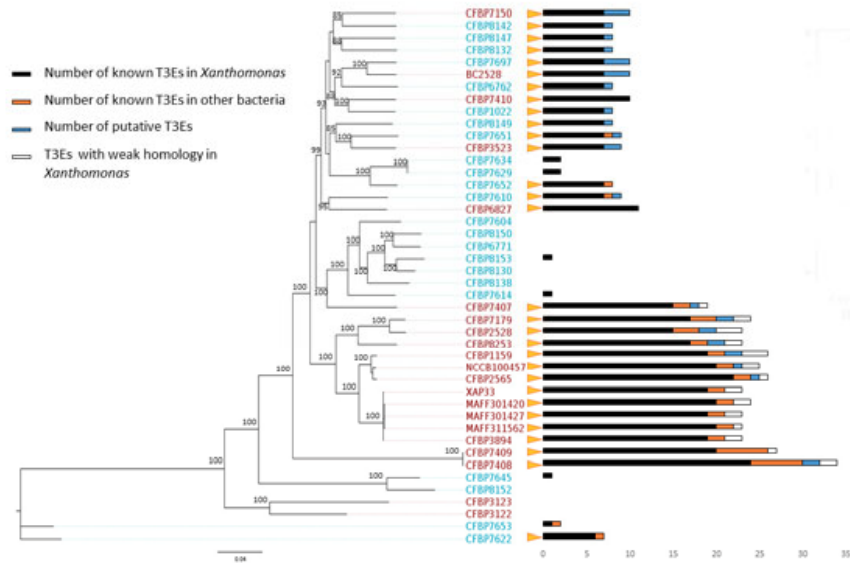
Fig. 4 Representation of T3E repertoires in *X. arboricola* strains. The phylogeny was performed in maximum likelihood using the concatenated sequences of 1,705 CDS composing the core genome of these 44 strains. Bootstrap values (100 bootstraps) higher than 85% are indicated at each node. Pathogenic strains are represented in red and commensal ones in blue. At the tip of each branch the orange triangles represent the presence of T3SS cluster and bars represent the composition of the T3E repertoire according to the legend.